Electron-phonon coupling in photoemission spectra

M. Hengsberger, R. Frésard, D. Purdie, P. Segovia, and Y. Baer
Institut de Physique, Université de Neuchâtel, CH-2000 Neuchâtel, Switzerland
(Received 13 April 1999)

We present high-resolution photoemission data of the $\overline{\Gamma}$-surface state on Be(0001). Near the Fermi surface a narrow quasiparticle peak caused by strong electron-phonon coupling emerges. A many-body calculation is performed, which describes precisely the exceptional evolution of the experimental spectra. We demonstrate that all the necessary parameters can be directly deduced from the experiment. [S0163-1829(99)00236-2]

I. INTRODUCTION

The great popularity of photoemission in the study of solids can be mainly attributed to the capacity of this technique to yield direct access to the energy and momentum of the occupied electronic states. This simple interpretation of the spectra relies on the assumption that the different interactions experienced by the electrons are sufficiently weak to allow an identification of the observed excitations with the single-particle description of the electrons in the initial state. The success of this approach for conventional solids has been demonstrated in numerous studies performed with medium energy and angular resolution. The recent technical improvements of photoemission have opened the possibility to make more detailed studies of quasiparticle line shapes in moderately correlated electron systems, and to analyze the spectral form successfully within the framework of Fermi liquid theory.[1,2] When the properties of a material are dominated by a very high electron correlation, as in heavy fermions,[3] or by some other unconventional interaction, as in high-temperature superconductors,[4] a straightforward interpretation of the photoemission data is no longer possible. Spectral functions calculated from many-body treatments reveal complex and extended structures. Nevertheless, it is usually possible to identify in some region of the spectrum a quasiparticle peak reminiscent of the single-particle concept. The most extreme situation is probably encoutered in one-dimensional systems, where this link is no longer tractable.[5] In order to observe the exceptional excitations directly related to unconventional behavior in photoemission spectra, it is essential to probe the system on the parameter scale (energy, momentum, and temperature) of the relevant interactions.

In the present study we show that a nearly free-electron-like surface state of Be(0001) is drastically modified by the electron-phonon interaction. As already pointed out in a recent publication,[6] the relevant energy scale for this interaction is the narrow energy range spanned by the phonon bandwidth below the Fermi energy E_F. The electron-phonon coupling mechanism has been well understood for three decades, and the corresponding spectral functions have been calculated.[7–12] We demonstrate that the dramatic evolution of the low-energy excitations in the photoemission spectra resulting from this interaction is well predicted by conventional many-body theory.

The well documented Be(0001) surface[13] offers favorable conditions for studying a nearly perfect two-dimensional (2D) electron gas. The very low density of states (DOS) at E_F in Be ensures a weak coupling of the surface with the bulk.[14] The projection of the bulk band structure onto the (0001)-surface Brillouin zone (SBZ) leaves broad unoccupied regions allowing the existence of a surface state at $\overline{\Gamma}$. This is represented in Fig. 1 as plot of spectra along the $\overline{\Gamma M}$ direction of the SBZ. The surface system is almost isotropic, as shown in measurements of the electron and phonon dispersion curves.[13,14] Earlier photoemission data of this state[15,16] are in good agreement with the theoretical calculations of the surface electronic structure,[17] but the spectra close to E_F were not sufficiently well resolved to reveal the exceptional line shape evolution analyzed in the present paper. However, two previous studies provide clear indications that this surface state interacts strongly with surface phonon modes: very high amplitudes of Friedel oscillations resulting from defect scattering have been observed with scanning tunneling microscopy (STM),[14] and a strong temperature dependence of the surface state linewidth has been extracted

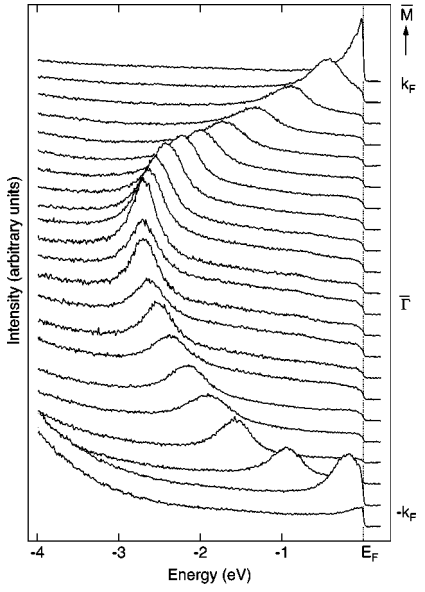

FIG. 1. Photoemission spectra of the $\overline{\Gamma}$ surface state on Be(0001) showing its parabolic dispersion along $\overline{\Gamma M}$. The spectra were recorded with unpolarized He I photons at 60 K. 0° corresponds to normal emission, and the angular resolution is 1°. The difference in angle between two neighboring spectra is 2.5°.

from photoemission data.[18] Our aim in this paper is to extend our recent presentation of high resolution photoemission spectra[6] of this surface state in the energy range where the electron-phonon interaction plays a dominant role. Moreover, we demonstrate that the data are very accurately predicted by the appropriate many-body formalism using realistic experimental parameters.

This work is organized as follows: in Sec. II, a simple model for the calculation of the spectral function is presented; experimental details are given in Sec. III; the comparison of theoretical predictions and the experimental spectra appears in Sec. IV; and, finally, Sec. V is the Conclusion.

II. THEORY

In a photoemission experiment, the sudden ejection of an electron from the ground state creates a hole, which can be selected according to its momentum k. The new state does not generally correspond to an eigenstate of the $(N-1)$-particle system and has to be projected onto all possible final eigenstates. Under the assumption that the optical matrix elements are constant, the energy distribution of the photoelectrons recorded in the experiment corresponds to the spectral function of the holes. If for some momentum value one final state dominates the spectral function, it is called a quasiparticle, appearing as a peak with Lorentzian shape in the spectra. Its linewidth corresponds to the inverse lifetime, its energy position to the energy of an elementary excitation from the ground state. These are given, respectively, by the imaginary part and the real part of the self-energy, which enters the calculation of the spectral function. A detailed description of the self-energy and its properties is beyond the scope of this work and can be found, for example, in Ref. 19.

A. Spectral function and momentum distribution

The spectral function $A(k,\omega)$ is given by the following general expression:

$$A(k,\omega)=\frac{|\mathrm{Im}\,\Sigma(k,\omega)|}{[\omega-E^0(k)-\mathrm{Re}\,\Sigma(k,\omega)]^2+[\mathrm{Im}\,\Sigma(k,\omega)]^2}, \tag{1}$$

where $E^0(k)$ is the band dispersion in the absence of interactions, and $\Sigma(k,\omega)$ the complex self-energy. Σ contains the whole many-body physics. In our particular case this comprises the electron-electron interaction, the electron-phonon interaction, and damping due to hole scattering at sample impurities and defects. To lowest order in the various interactions, the different contributions are simply summed up:[19]

$$\Sigma=\Sigma^{\mathrm{ph}}+\Sigma^{\mathrm{el\text{-}el}}+\Sigma^{\mathrm{imp}}. \tag{2}$$

The isolation of the interesting electron-phonon term Σ^{ph} is a rather difficult task, because it necessitates an *a priori* estimation of the last two contributions. However, in the present situation, the conditions are favourable and offer a simple way to circumvent this difficulty. First, the impurity term is purely imaginary and nearly constant in the small energy range of interest.[20] Second, the real part of the electron-electron term can be linearized close to the Fermi level on the scale of the electron bandwidth,[1] leading to a constant change in the Fermi velocity v_F. If the experimentally observed dispersion $E(k)=\hbar v_F\times(k-k_F)$ is extrapolated from binding energies higher than the phonon bandwidth but small with respect to the electron bandwidth, $\mathrm{Re}\,\Sigma^{\mathrm{el\text{-}el}}$ is taken into account: $E(k)=E^0(k)+\mathrm{Re}\,\Sigma^{\mathrm{el\text{-}el}}(k,\omega)$. In order to implement the imaginary parts, a parameter $\Delta(k)=\mathrm{Im}\,\Sigma^{\mathrm{el\text{-}el}}[k,\omega=E(k)]+\mathrm{Im}\,\Sigma^{\mathrm{imp}}$ is introduced, which is used in the first step of the analysis as a fitting parameter of the spectral function to the momentum resolved spectra. Δ depends on energy through $E(k)$. The electron-electron contribution can be calculated in two dimensions to yield:[21]

$$\mathrm{Im}\,\Sigma^{\mathrm{el\text{-}el}}(k,\omega)\propto\omega^2\left[1+0.53\left|\ln\left(\frac{\omega}{E_F}\right)\right|\right], \tag{3}$$

where ω is measured from E_F. Equation (3) results in an almost parabolic function. When analyzing the experimental data, this function cannot be distinguished from the well-known quadratic dependence in three dimensions.[19,22] The proportionality factor can be related to the electron density and the plasmon energy,[1,22] but this link is much less evident in two dimensions than in three. We will therefore analyze our data using both the 2D and the 3D formalisms. The resulting energy dependence of $\Delta[E(k)]$ should reflect Eq. (3), with the addition of a constant term accounting for impurity scattering. Equation (2) leads then to

$$\Sigma(k,\omega)=\Sigma^{\mathrm{ph}}(k,\omega)+i\Delta(k), \tag{4}$$

which is inserted into Eq. (1).

The momentum distribution $n(k,T)$ can be obtained by integrating $A(k,\omega,T)f(\omega,T)$ over all energies ω,f being the Fermi function.[23] For $T=0$, $n(k)$ exhibits a discontinuity at k_F of the height of the quasiparticle weight Z. In a noninteracting electron system, Z is 1 and $n(k)$ reduces to the usual Fermi function. In the presence of interactions, the Fermi velocity is diminished by a factor of $Z=1/(1+\gamma)$, where γ is the renormalization constant or enhancement factor of the effective mass. Since the electron-electron contribution is already taken into account in our case, we are allowed to equate the measured renormalization γ to the electron-phonon coupling parameter λ.[6]

B. Electron-phonon coupling

In an isotropic system, the electron-phonon part of the self-energy can be well approximated by averaging the electron-phonon coupling function over the Fermi surface.[10] The phonon modes then enter into the calculation through the so-called McMillan or Eliashberg function $\alpha^2F(\tilde{\omega})$, approximated here as a product of the coupling strength and the phonon DOS. The latter is taken to be linear in energy in two dimensions. The coupling strength is a smooth function of energy[10,24] and is taken here to be constant. The basic idea of our approach is, therefore, the linearization of the Eliashberg function submitted to the constraint that the maximum phonon energy equals the experimentally observed value

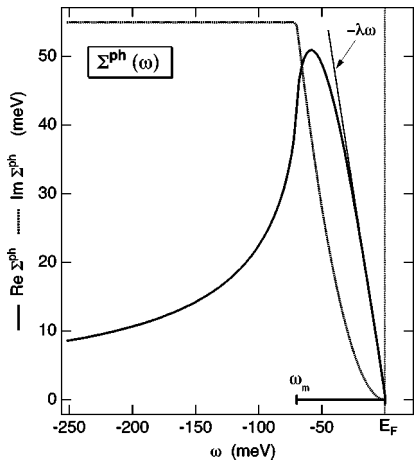

FIG. 2. Plot of the electron-phonon part of the self-energy used in this work (see text). The real and the imaginary part are shown as thick solid and dotted lines, respectively. The real part can be linearized near E_F (thin solid line). The experimentally derived maximum phonon energy is 70 meV (Ref. 25) (indicated by a stick), and the coupling parameter λ equals 1.18.

ω_m.[13,25] It is this value which sets the relevant energy scale of the interaction.[6] The value of the coupling parameter λ, which is defined by the following integral:[26]

$$\lambda = 2\int_0^{\omega_m} \frac{\alpha^2 F(\tilde{\omega})}{\tilde{\omega}} d\tilde{\omega}, \tag{5}$$

then gives $\alpha^2 F(\tilde{\omega})$. The experimental value of λ is obtained from photoemission data either as the renormalization factor of the band dispersion at E_F[6] or, equivalently, from the temperature dependence of the surface state linewidth near the Fermi surface.[18] A straightforward evaluation of Eq. (5) yields then $\alpha^2 F(\tilde{\omega}) = \lambda\tilde{\omega}/(2\omega_m)$.

Since the self-energy is only weakly k dependent, $\Sigma^{ph}(k,\omega)$ can be replaced by its value at k_F.[7] One then arrives at the standard expression, dropping the index k_F (Ref. 10)

$$\Sigma^{ph}(\omega) = \int_{-E_F}^{\infty} d\epsilon \int_0^{\omega_m} d\tilde{\omega}\, \alpha^2 F(\tilde{\omega}) \left\{ \frac{1-f(\epsilon,T)+N(\tilde{\omega},T)}{\omega-\epsilon-\tilde{\omega}+i\delta^{\pm}} + \frac{f(\epsilon,T)+N(\tilde{\omega},T)}{\omega-\epsilon+\tilde{\omega}+i\delta^{\pm}} \right\}, \tag{6}$$

where $f(\epsilon,T)$ and $N(\tilde{\omega},T)$ are the Fermi-Dirac and Bose-Einstein factors, respectively. $\omega=0$ refers to the Fermi energy, and $\delta^{\pm} \equiv \mathrm{sgn}(\omega)\,\delta$ is an infinitesimal number. Assuming particle-hole symmetry, the limits of the ϵ integration are set to $\pm E_F$. Σ^{ph} from Eq. (6) at $T=0$ is displayed in Fig. 2. Its behavior is strongly reminiscent to results of other calculations[8–10] except for the imaginary part in the limit $\omega \to 0$. In contrast to calculations in three dimensions, where $\mathrm{Im}\,\Sigma^{ph}$ has a ω^3 dependence,[8] the 2D results reveal a ω^2 law. The real part shows the expected linear dependence with slope $-\lambda$ and vanishes at E_F according to Luttinger's theorem.[27] At energies further than the maximum phonon frequency from E_F, the real part decreases towards zero, whereas the imaginary part remains constant and vanishes for $|\omega| > E_F$. The strong influence of the electron-phonon coupling on the structure of the spectral function is thus seen to be confined to a small energy region of the order of ω_m around the Fermi surface.

III. EXPERIMENT

The sample was mechanically polished prior to insertion into vacuum, where it was treated with standard cycles of sputtering and annealing.[6] The surface exhibited the expected hexagonal low-energy-electron diffraction pattern. For the photoemission experiment, two separate He discharge lamps can be used as light source. One of these is connected by a quartz capillary to the measurement chamber, and the second one through a double-focusing monochromator, which produces a linearly polarized output with an efficiency greater than 90%. The angle between both incident light beams and the analyzer axis is fixed to 45°. The total spectrometer energy resolution is better than 5 meV. The angular resolution was set to 0.2° in the direction of the strong dispersion (except when otherwise stated) and 0.5 $-1°$ perpendicular to it.[6] The relevant k-space resolution at k_F is $\delta k \approx 0.009$ Å^{-1}. All spectra presented here are taken with He I-photons (21.2 eV). The emission angle is varied by rotation of the sample.

In a photoemission process, only the component of the electron wave vector parallel to the surface is conserved, and this can easily be calculated for a given emission angle and kinetic energy.[28] Surface states have a truly 2D behavior, i.e., no dispersion perpendicular to the surface. The advantage for our experiment is twofold: the wave vector of the photohole is known exactly, and the width of an observed peak originates exclusively from the lifetime of the photohole.[28] In Fig. 1, a set of spectra is shown, covering the whole band dispersion along $\overline{\Gamma M}$. The spectra were recorded with an angular resolution of 1° at a sample temperature of 60 K, using He I-photons from the unmonochromatized source. An analysis yields the following band parameters for $\overline{\Gamma M}$ ($\overline{\Gamma K}$): a parabolic dispersion with an effective mass of 1.19 (1.14) times the electron rest mass, and a Fermi wavevector of 0.924 Å^{-1} (0.90 Å^{-1}). The occupied bandwidth was found to be 2.73 eV, in good agreement with published data.[15,16] Due to the even symmetry of the surface state wave function with respect to the measurement plane,[15] the state is only observed when excited by p-polarized light, i.e., with the vector potential lying within this plane.

IV. RESULTS AND DISCUSSION

Figure 3 displays spectra (dots) taken for $T=12$ K in a narrow range around k_F along $\overline{\Gamma K}$. They are labeled by the wave vector $k(E_F)$ with respect to k_F and numbered for the sake of simplicity. The spectra along $\overline{\Gamma M}$ (Fig. 4) were already presented in detail in a recent publication.[6] All curves are normalized to the integrated photon flux. The evolution of the spectra is the same for $\overline{\Gamma K}$ and for $\overline{\Gamma M}$.[6] As the surface state approaches E_F (spectra 1–6 in Fig. 3), a second peak appears at -70 meV. Its intensity increases dramati-

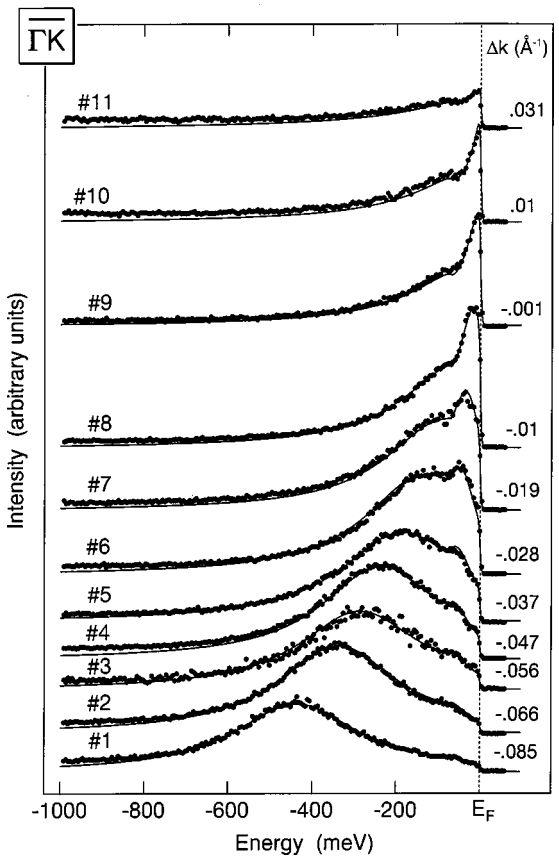

FIG. 3. Photoemission spectra (12 K, *p*-polarized He I photons) of the surface state near E_F in the direction $\overline{\Gamma K}$ (dots), compared to the spectral functions, calculated for the corresponding emission angles (lines). Spectra are numbered and labeled with the corresponding wave vectors $\Delta k = k(E_F) - k_F$; k was calculated here for emission from the Fermi level. The range in emission angle covered by these spectra is 3°.

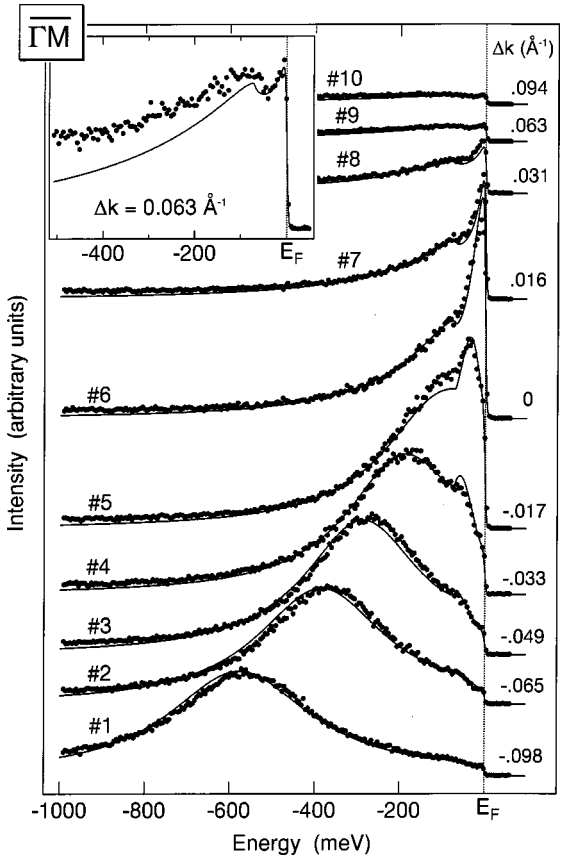

FIG. 4. As in Fig. 3, but with the wave vector along $\overline{\Gamma M}$. The spectra extend over 6°. Inset: spectrum No. 9, enhanced in order to show the sharp peak pinned at E_F.

cally towards k_F, where it finally dominates the spectral function (No. 8). For $k > k_F$ (No. 9 to 11 in Fig. 3), the whole spectral intensity decreases rapidly. However, the spectra show a sharp peak remaining pinned at E_F and a second weak structure at about -70 meV (see inset of Fig. 4). The same line shapes can be observed around $-k_F$ and in the corresponding spectra excited with He II-radiation (40.8 eV, spectra not shown).

In order to simulate the photoemission line shapes, we adopt the procedure described in Sec. II with the following parameters: $\omega_m = 70$ meV was taken from electron-energy-loss measurements,[13,25] and $\lambda = 1.18$ was determined by comparison of the quasiparticle dispersions in the present spectra.[6] The high Debye temperature of the sample (~ 1000 K) with respect to the sample temperature (12 K) allows us to compare the experimental spectra with calculations performed for $T = 0$. The Eliashberg coupling function and the phonon contribution to the self-energy are evaluated using Eqs. (5) and (6). k is fixed by the experiment and $E(k)$ is given by extrapolation. With Δ as the only variable parameter, $A(k,\omega)$ is calculated from Eqs. (1) and (4) and multiplied by the Fermi function at 12 K. The resulting spectrum is then convoluted in k-space with a Gaussian of width δk to account for the experimental angular resolution, the energy resolution being neglected. The intensity of each calculated spectrum is adjusted to the experimental counterpart by multiplication with a factor, found to vary only slightly with k (standard deviation 10%; see upper panel in Fig. 5). This underlines the stability of the experimental conditions and the reproducibility of the spectra, which were recorded over a period of several weeks. The final results are superimposed as lines in Figs. 3 and 4 in order to facilitate comparison. The calculation reproduces almost perfectly the double structure and the intensity ratio between the two main peaks. It is interesting to notice that the sharp peak at E_F for $k > k_F$ does not appear in the spectral function of the pure electron-phonon system, in contrast to the weak structure at slightly higher binding energies (at $\sim \omega_m$, see inset in Fig. 4). It was found to be the remnant of the strong quasiparticle peak, centered far above E_F and broadened by Δ. It serves, thereby, as a sensitive probe for the fitting procedure.

In the lower panel of Fig. 5 the theoretical momentum distribution $n(k)$ at $T = 0$, obtained by integration of the spectral function according to Sec. II, is plotted. Curve (a), calculated for the pure electron-phonon coupling, exhibits the expected discontinuity of height $Z = 1/(1+\lambda)$ at k_F. Curve (b) takes both the experimental resolution and the parameter $\Delta(k)$ into account, the latter coming from the results of the line-shape fits (see below). The experimental values, obtained by integration of the photoemission spectra, are given by the symbols in the plot. The raw spectra have been used without any adjustment of their relative intensities. The errors due to the cutoff of the spectra at high binding ener-

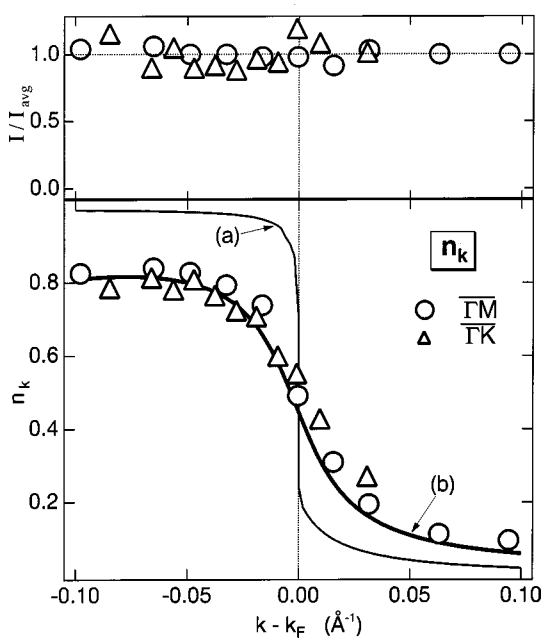

FIG. 5. Upper panel: intensity values used to adjust the calculations to the experimental spectra of Figs. 3 (open triangles) and 4 (open circles). Lower panel: a comparison of experimental values (symbols) and theory (solid lines) for the momentum distribution $n(k)$. The thin line (a) is calculated for $T=0$, $\Delta=0$ and infinite angular resolution, the thick line (b) for $T=0$, $\Delta(k)$ (from the fit results) and a resolution of 0.2°.

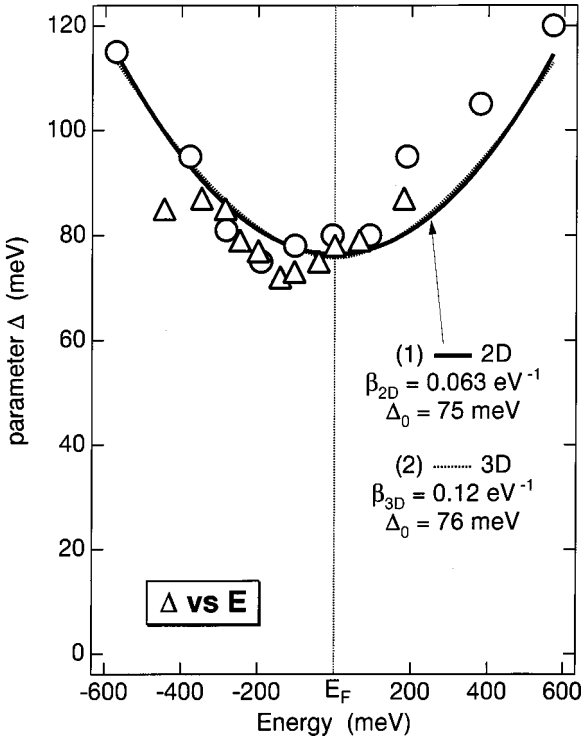

FIG. 6. Plot of the fit parameter Δ versus E; symbols like in Fig. 5. The lines are fits using a two-dimensional (curve 1, thick line) and a three-dimensional (curve 2, thin line) model (see text for detail).

gies and the inelastic background were found to be small, compared to the error radius of the experimental normalization procedure. The discontinuity is smeared out, but the intensity excess above k_F, typical for an interacting fermion system, is clearly reproduced.

Keeping in mind that the only fit parameter used is Δ, the overall agreement between the experimental data and the results of our simple model is excellent. The physical meaning of Δ becomes clearer if one plots the values obtained as a function of the band energy E (Fig. 6). As anticipated in Sec. II, this term can be decomposed into a constant offset value $\Delta_0=75$ meV and a pseudoparabolic function (with curvature β). Figure 6 demonstrates that this functional form of Δ is a good approximation of the experimental values, and that only two parameters, Δ_0 and β, are sufficient to fit the whole set of spectra. Using Eq. (3), a value of 0.063 eV^{-1} is found for the prefactor β_{2D} [curve (1) in Fig. 6], whereas the calculation in three dimensions yields $\beta_{3D}=0.12$ eV^{-1} [curve (2)]. Following the interpretation given in Ref. 1, the plasmon energy of the Coulomb gas can be derived from β_{3D}. A value of 13.3 eV is obtained from our analysis, which compares favorably with both bulk and surface plasmon energies of Be (19.5 eV and 11.3 eV, respectively[29]). A well founded prediction for Δ_0 is more speculative. The contribution of the electron-electron and electron-phonon interactions due to the finite measurement temperature are less than 1 meV and can, therefore, be neglected.[30] Scattering due to surface disorder and impurities is taken to be the dominant mechanism. Δ_0 can be translated into a mean-free path λ_{mfp} of about 15 Å in the surface plane. Previous photoemission studies reveal values for the linewidth similar to our room temperature data, both at $\overline{\Gamma}$ and near E_F.[16,18] Such a correspondence can hardly be accidental and seems to indicate an inherent limitation of the quality of the Be(0001)-surface resulting from the preparation.

For the electron-phonon coupling, the description of the observed peaks in terms of quasiparticles is only reliable for

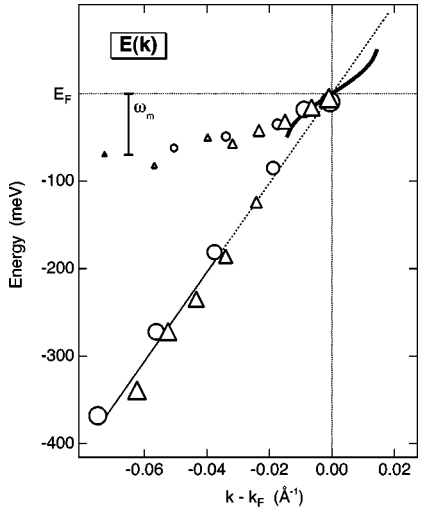

FIG. 7. Comparison of the positions of the peak maxima, observed along $\overline{\Gamma M}$ and $\overline{\Gamma K}$ (symbols as in Fig. 5) with the calculated quasi-particle dispersions. The solid/dashed line corresponds to $E(k)$ in absence of the electron-phonon coupling, and the thick line to the dispersion renormalized by the electron-phonon interaction, $ZE(k)$. The size of the symbols reflects the intensity of the corresponding peaks.

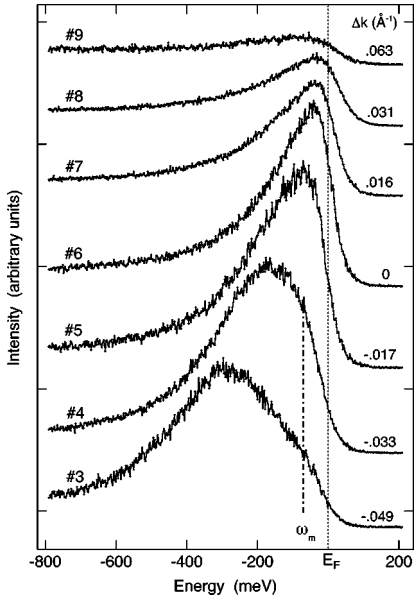

FIG. 8. Spectra taken around k_F along $\overline{\Gamma M}$ at 300 K (He I, p polarized). The numbers correspond to those in Fig. 4. The maximum phonon frequency is indicated by a vertical dashed-dotted line.

energies either very close to E_F, or substantially further than ω_{m} from E_F.[8,10] For the intermediate region, a two-peak structure is observed reflecting the interplay of different excitation channels, and the calculated spectra no longer account for elementary excitations. In order to illustrate this, we show the quasiparticle dispersions in Fig. 7 together with the positions of the experimental peak maxima. The thin solid line denotes the dispersion of the band $E(k)$ in the energy range where only the electron-electron interaction plays a role and the quasiparticle description is adequate. Its dashed continuation toward k_F is the extrapolation used in the calculation. The thick solid line near k_F is the quasiparticle dispersion lowered by the electron-phonon coupling $ZE(k)$. Superimposed as symbols are the experimental points for both directions, $\overline{\Gamma M}$ and $\overline{\Gamma K}$. The size of the symbols scales with the relative intensities of the peaks. It is obvious that the experimental points follow the quasiparticle dispersion at E_F only in a small range below the Fermi energy, where the corresponding peak dominates the spectral function. Its weight causes an important enhancement of the DOS at E_F and confirms, thereby, the conclusion reached without explicit calculation in the first paper.[6]

As a last point, we show in Fig. 8 a collection of spectra taken at a sample temperature of 300 K along $\overline{\Gamma M}$, the spectra being labeled accordingly to Fig. 4. Two features are conspicious. Firstly, the two bottommost spectra (Nos. 3 and 4) cannot be fitted with a single Lorentzian but exhibit shoulders at approximately ω_{m}, indicated by a vertical dashed-dotted line in Fig. 8. Hence, at high temperature the coupling to surface phonons markedly influences the spectral function, even though it is smeared out by the broadening of the Fermi function. Secondly, in the spectra for $k > k_F$ (Nos. 7–10), the point of half-intensity of the spectral cutoff is located some 20–30 meV *above* the Fermi energy. This thermal population of states directly above E_F demonstrates that the surface state dispersion is continuous across the Fermi energy. We have verified that when these spectra are divided by the Fermi function for 300 K, the peak maxima follow the same quasiparticle dispersion as in the occupied part. This observation rules out any interpretation of these data in terms of other mechanisms, like superconductivity or charge density waves, which imply the opening of a gap with concomitant accumulation of states below E_F.[6]

V. SUMMARY AND CONCLUSION

Our data demonstrate that the photoemission spectra of the $\overline{\Gamma}$ surface state on Be(0001) are progressively dominated by the electron-phonon interaction as the state approaches and crosses the Fermi surface. This remarkable behavior is interpreted within a many-body framework, which includes all relevant interactions determining the spectral function. In addition to the instrumental conditions, two parameters imposed by independent experiments are used: the dispersion of the surface state without electron-phonon coupling is given by extrapolation from the spectra measured at binding energies larger than the surface phonon bandwidth ω_{m}, and ω_{m} is taken from electron-energy-loss data.[25] The Eliashberg coupling function is approximated by a linear function in energy, and, as a consequence, the electron-phonon interaction is determined in a simple way by the coupling parameter λ. The energy dependence of the inverse lifetime resulting from electron-electron scattering contains only the unknown factor β. Finally, electron scattering due to sample imperfections is accounted for by a constant term Δ_0. The fit of the spectral functions to the whole set of photoemission spectra is performed by adjusting exclusively the three parameters λ, β, and Δ_0, and reliable values are obtained. In particular, the large electron-phonon coupling explains the origin of the unusual STM images observed on this surface.[14] Despite the stringent conditions imposed in the fitting procedure, theory provides an exceptionally good prediction of the spectral shape evolution and momentum distribution.

Recently, we became aware of similar work by LaShell and co-workers.[31] They obtain $\lambda = 0.7 \pm 0.1$ for the Be(0001) surface state using a different approach. Despite the difference in the coupling parameter, their results are in general agreement with ours and thus confirm the physical correctness of the analysis.

In conclusion, we have shown that this many-body treatment provides an adequate framework for describing the strong electron-phonon interaction in two dimensions. The nearly perfect reproduction of the full set of experimental spectra by the calculations demonstrates that the fundamental parameters underlying the different interactions can be extracted from the photoemission spectra with a high degree of confidence.

ACKNOWLEDGMENTS

We are indebted to H. Beck for stimulating discussions, and to M. Garnier for his help during the first measurements. The work was funded by the Fonds National Suisse de la Recherche Scientifique.

[1] R. Claessen, R. O. Anderson, J. W. Allen, C. G. Olson, C. Janowitz, W. P. Ellis, S. Harm, M. Kalning, R. Manzke, and M. Skibowski, Phys. Rev. Lett. **69**, 808 (1992).
[2] J.W. Allen, G.-H. Gweon, R. Claessen, and K. Matho, J. Phys. Chem. Solids **56**, 1849 (1995).
[3] M. Garnier *et al.*, Phys. Rev. Lett. **78**, 4127 (1997).
[4] J.C. Campuzano, H. Ding, M. R. Norman, M. Randeria, A. F. Bellman, T. Yokoya, T. Takahashi, H. Katayama-Yoshida, T. Mochiku, and K. Kadowaki, Phys. Rev. B **53**, R14 737 (1996); Z.-X. Shen and J.R. Schrieffer, Phys. Rev. Lett. **78**, 1771 (1997); M.R. Norman, H. Ding, J. C. Campuzano, T. Takeuchi, M. Randeria, T. Yokoya, T. Takahashi, T. Mochiku, and K. Kadowaki, *ibid.* **79**, 3506 (1997).
[5] B. Dardel, D. Malterre, M. Grioni, P. Weibel, and Y. Baer, Phys. Rev. Lett. **67**, 3144 (1991).
[6] M. Hengsberger *et al.*, Phys. Rev. Lett. **83**, 592 (1999).
[7] A.B. Migdal, Zh. Éksp. Teor. Fiz. **34**, 1438 (1958) [Sov. Phys. JETP **7**, 996 (1958)].
[8] S. Engelsberg and J.R. Schrieffer, Phys. Rev. **131**, 993 (1963).
[9] G. Grimvall, Phys. Kondens. Mater. **6**, 15 (1967).
[10] G. Grimvall, Phys. Kondens. Mater. **9**, 283 (1969).
[11] V. Meden, K. Schönhammer, and O. Gunnarsson, Phys. Rev. B **50**, 11 179 (1994).
[12] O. Gunnarsson, H. Handschuh, P. S. Bechthold, B. Kessler, G. Ganteför, and W. Eberhardt, Phys. Rev. Lett. **74**, 1875 (1995).
[13] E.W. Plummer and J.B. Hannon, Prog. Surf. Sci. **46**, 149 (1994).
[14] P.T. Sprunger, L. Petersen, E. W. Plummer, E. Laegsgaard, and F. Besenbacher, Science **275**, 1764 (1997).
[15] U.O. Karlsson, S. A. Flodström, R. Engelhardt, W. Gädeke, and E. E. Koch, Solid State Commun. **49**, 711 (1984).
[16] R.A. Bartynski, E. Jensen, T. Gustafsson, and E.W. Plummer, Phys. Rev. B **32**, 1921 (1985).
[17] E.V. Chulkov, V.M. Silkin, and E.N. Shirykalov, Surf. Sci. **188**, 287 (1987).
[18] T. Balasubramanian, E. Jensen, X.L. Wu, and S.L. Hulbert, Phys. Rev. B **57**, R6866 (1998).
[19] L. Hedin and S. Lundqvist, in *Solid State Physics: Advances in Research and Applications*, edited by F. Seitz, D. Turnbull, and H. Ehrenreich (Academic, New York, 1969), Vol. 23.
[20] A. Beckmann, K. Meinel, M. Heiler, Ch. Ammer, and H. Neddermeyer, Phys. Status Solidi B **198**, 665 (1996).
[21] C. Hodges, H. Smith, and J.W. Wilkins, Phys. Rev. B **4**, 302 (1971).
[22] J.J. Quinn and R.A. Ferrell, Phys. Rev. **112**, 812 (1958).
[23] The photoemission spectrum is given by $\mathrm{Im}\,G^{<}(k,\omega) = \mathrm{Im}\,G^{av}(k,\omega)f(\omega)$. The imaginary part of the advanced Green's function $G^{av}(k,\omega)$ corresponds to the spectral function in Eq. (1).
[24] S.Y. Savrasov and D.Y. Savrasov, Phys. Rev. B **54**, 16 487 (1996).
[25] J.B. Hannon and E.W. Plummer, J. Electron Spectrosc. Relat. Phenom. **64/65**, 683 (1993).
[26] G. Rickayzen in *Techniques of Physics*, edited by N.H. March and H. N. Daglish (Academic Press, London, 1980), Vol. 5.
[27] J.M. Luttinger, Phys. Rev. **119**, 1153 (1960).
[28] N.V. Smith, P. Thiry, and Y. Petroff, Phys. Rev. B **47**, 15 476 (1993).
[29] H. Höchst, P. Steiner, and S. Hüfner, Phys. Lett. **60A**, 69 (1977).
[30] The contribution of the electron-phonon part at $\omega=0$ and $T>0$ can be estimated to leading order in the Sommerfeld expansion of Eq. (6) to be of the order of $(k_BT)^2/\omega_m$. The electron-electron interaction was calculated for finite temperature in Ref. 21.
[31] S. LaShell, E. Jensen, and T. Balasubramanian (unpublished).